Available online at www.sciencedirect.com

SciVerse ScienceDirect

Mathematics and Computers in Simulation 82 (2011) 590–603

MATHEMATICS AND COMPUTERS IN SIMULATION

www.elsevier.com/locate/matcom

Original articles

Synchronization of coupled chaotic FitzHugh–Nagumo neurons via Lyapunov functions

Le Hoa Nguyen [a,1], Keum-Shik Hong [b,*]

[a] School of Mechanical Engineering, Pusan National University, 30 Jangjeon-dong, Gumjeong-gu, Busan 609-735, Republic of Korea
[b] Department of Cogno-Mechatronics Engineering and School of Mechanical Engineering, Pusan National University, 30 Jangjeon-dong, Gumjeong-gu, Busan 609-735, Republic of Korea

Received 13 June 2011; received in revised form 28 September 2011; accepted 14 October 2011
Available online 28 October 2011

Abstract

After investigating the effect of the frequency of an external electrical stimulation on the chaotic dynamics of a single FitzHugh–Nagumo (FHN) neuron, this paper derives both a sufficient and a necessary condition of the coupling coefficient for self-synchronization of two interacting FHN neurons by using the Lyapunov function method and the largest transverse Lyapunov exponent, respectively. Also, for the cases that self-synchronization is not achieved through the coupling coefficient, a feedback control law for synchronization using the Lyapunov method is investigated. The performance of the proposed control law is compared with that of an existing one in the literature. Simulation results are provided.

Keywords: Synchronization; Coupling coefficient; FitzHugh–Nagumo model; Lyapunov function; Nonlinear control

1. Introduction

Chaos as a complicated nonlinear phenomenon has attracted very considerable interest and attention over the past three decades in many scientific disciplines including physics, chemistry, ecology, biology, and others. The interest in chaotic systems lies in their complexity, unpredictable behavior and high sensitivity to initial conditions and parameter variations. In biological systems, chaotic and other complex behaviors such as bifurcation, periodic, and quasi-periodic oscillations have been observed in various experiments of current-stimulated excitable cells [9,19,26]. In 1952, Hodgkin and Huxley proposed a four-dimensional mathematical model that approximates the electrical characteristics of excitable cells [22]. Since then, chaotic oscillations and routes to chaos that are observed in real biological neurons have been successfully described quantitatively with the Hodgkin–Huxley model [2]. Based on the Hodgkin–Huxley equations, various three-dimensional models of excitable cells that exhibit bursting behavior were proposed [11,21,27,35], and chaotic bursting behavior as well as the bifurcation diagram structure of such cells have been studied in [13,17,29]. A more reduced model consisting of two first-order differential equations was formulated by FitzHugh [18], and its equivalent circuit was created by Nagumo et al. [30]. When the FitzHugh–Nagumo (FHN)

* Corresponding author. Tel.: +82 51 510 2454; fax: +82 51 514 0685.
E-mail addresses: nglehoa@pusan.ac.kr (L.H. Nguyen), kshong@pusan.ac.kr (K.-S. Hong).
[1] Tel.: +82 51 510 2973.

0378-4754/$36.00 © 2011 IMACS. Published by Elsevier B.V. All rights reserved.
doi:10.1016/j.matcom.2011.10.005

system is space-clamped and subjected to a stimulating electrical current, a variety of complex dynamical behavior such as phase-locked limit cycles, quasi-periodicity, and chaos are observed [12,44]. Individual neurons can exhibit irregular behavior, whereas ensembles of neurons might be synchronized in order to transmit biological information or to produce regular and rhythmical activities [16]. The study of synchronization processes for populations of interacting neurons is basic to the understanding of some key issues in neuroscience. Recently, many researchers have focused on the synchronization of coupled neurons, which is one of the fundamental issues in understanding the neuronal behaviors in networks (see [3,10,14,15,31,36–39,45,47] and the references therein).

In the past years, the synchronization of coupled chaotic systems has been intensively studied by a large number of authors [5,7,33,34,40–42,49], and many complex synchronization phenomena such as riddled basin, riddling bifurcation, blowout bifurcation, and on–off intermittency have been reported [4,32]. The conditions of the coupling strength for synchronization, the influence of noise, and the effects of a parameter mismatch on the synchronization of coupled chaotic systems have been also investigated [40,50].

For the problem of synchronizing two coupled neurons, many studies have confirmed that when the intensity of an internal noise exceeds a critical value, the self-synchronization can be achieved [10,31,37]. Other numerical results [38,50] have shown that strong coupling can also synchronize a system of two coupled neurons. Also, various methods using modern control theories have been proposed to synchronize two chaotic systems (see [3,8,14,15,25,28,38,39,43,45–47] and the references therein). Cornejo-Pérez and Femat [14] investigated the synchronization of two noiseless Hodgkin–Huxley neurons using a modified feedback control law with a high-gain observer. Deng et al. [15] used a backstepping control law to synchronize two coupled chaotic FHN neurons under external electrical stimulation. The same chaotic neuron system could be also synchronized using an H_∞ variable universe adaptive fuzzy control [47] or a nonlinear robust adaptive control [39]. In the work of Tian et al. [45], a linearizing control law in association with a dynamic uncertainty estimator was designed to synchronize two Hodgkin–Huxley neurons exposed to external periodic stimulation and extremely low frequency electric field.

In the present paper, first, the dynamic behavior of a FHN neuron stimulated by an external electrical signal is investigated. By introducing the bifurcation diagram and the largest Lyapunov exponent, the effect of the external electrical stimulation's frequency on the chaotic behavior of the neuron is fully investigated. Second, by using the Lyapunov function method and calculating the largest transverse Lyapunov exponent, respectively, a sufficient condition and a necessary condition of the coupling coefficient for achieving self-synchronization between two coupled chaotic FHN neurons are established. Third, for the cases that the coupling coefficient does not satisfy the self-synchronization conditions, a new feedback control law (based on the Lyapunov method) that achieves synchronization of two chaotic neurons is proposed. The proposed control law can be extended to the cases that the external electrical stimulations applied to each neuron are different. Our method, compared with the work in [15], provides a much improved control performance: With the proposed control law, synchronization was achieved at $t \approx 15$ (dimensionless), whereas it was achieved with the control law proposed in [15] at $t > 100$.

This paper is organized as follows. In Section 2, the dynamics of a single FHN neuron under various external electrical stimulations are investigated. In Section 3, a sufficient condition and a necessary condition of the coupling coefficient for the achievement of global self-synchronization are analyzed. The design of a feedback control law for synchronization, when the coupling coefficient does not satisfy the self-synchronization conditions, is also addressed in this section. Finally, conclusions are drawn in Section 4.

2. Dynamics of a single FHN neuron

2.1. Model description

The FHN model, a simplified version from the Hodgkin–Huxley model [18], is a genetic model for active membranes. Its justification is based in the observed fact that the membrane voltage and the activation of sodium current vary in a similar time scale, whereas the inactivation of sodium current and the activation of potassium current change in much slower time scale. The FHN neuron equations are

$$\frac{dx}{dt} = x(x-1)(1-b_1 x) - y + s(t), \tag{1a}$$

$$\frac{dy}{dt} = b_2 x, \tag{1b}$$

where x represents the membrane voltage and y represents the recovery variable. It is noted that the equations are rescaled ones from the actual membrane voltage V and the actual recovery variable W by the peak value of the active potentials V_{peak} (i.e., $x = V/V_{peak}$, $y = W/V_{peak}$). Also, $b_1 = V_{peak}/V_{th}$, where V_{th} is the threshold membrane voltage, and b_2 is a positive constant. The external electrical stimulation $s(t)$ is given by

$$s(t) = \frac{a}{2\pi f} \cos\ 2\pi f t, \tag{2}$$

where a and f are dimensionless parameters presenting, respectively, the amplitude and the frequency of the applied electrical stimulus. As the frequency or amplitude of the stimulation is changed, periodic or chaotic oscillations of the membrane voltage are observed. The periodic oscillations are classified as m:n phase-locking rhythms, where m and n are the number of actual spikes and the number of regularly timed stimuli realized in one response period, respectively (therefore nT is the period of the response if T is the period of the stimulation). The 1:1 phase-locking rhythms mean that the membrane voltages respond synchronously to the stimuli. Fig. 1 shows various dynamic behaviors of the FHN neuron (1) stimulated by the external electrical stimulation in (2), in which the time series of the membrane voltages x and the x–y phase portraits for some values of f and a are given.

2.2. Chaotic behavior

In order to investigate the chaotic behavior of (1), the bifurcation diagrams and the variation of the largest Lyapunov exponents are explored. The bifurcation diagrams are constructed using a Poincaré section (Σ: $x + 0.045 = 0$ and $dy/dt > 0$) in the phase space, which can capture all the spikes/orbits generated by (1). The largest Lyapunov exponents are computed using the method described in [48]. For an n-dimensional continuous dynamic system, the largest Lyapunov exponent is defined as

$$\lambda_{max} = \lim_{t \to +\infty} \frac{1}{t} \log \frac{\delta(t)}{\delta(0)}, \tag{3}$$

where $\delta(t)$ is the principal axis of the n-ellipsoid generated by an infinitesimal n-sphere of initial conditions. If $\lambda_{max} > 0$, the system is chaotic. Otherwise, the system follows a limit cycle or is quasi-periodic [1,48]. The fourth-order Runge–Kutta algorithm is used to numerically integrate (1) with a diminishing step-size $\Delta t = 0.005$. Here, we fix the parameters as $b_1 = 10$, $b_2 = 1.0$, $a = 0.1$ and use the frequency f of the external electrical stimulation as a bifurcation parameter.

Fig. 2 shows the bifurcation diagram (upper) and the corresponding variation of the largest Lyapunov exponent (lower) of the periodically stimulated FHN neuron over the frequency range $0.06 < f < 0.17$. As shown in Fig. 2, a rich dynamic behavior is observed. For large frequencies ($f > 0.1625$), the neuron Exhibits 0:1 phase-locking rhythms. The membrane voltages are suppressed entirely, leaving only sub-threshold oscillations. The 1:2 phase-locking rhythms can be found for $0.078 < f < 0.095$ and $0.131 < f < 0.1609$. The neuron responds synchronously (1:1 phase-locking rhythms) to the stimuli for $f < 0.067$ and $0.095 < f < 0.1245$. It can also be seen from Fig. 2 that three chaotic regions are found and they are denoted by (I), (II) and (III) sequentially. These chaotic regions are confirmed by the positive values of the largest Lyapunov exponents (the lower part of Fig. 2). The magnification of the chaotic regions and their corresponding largest Lyapunov exponent are depicted in Fig. 3. The chaotic region (I) appears in the middle of 0:1 and 1:2 phase-locking rhythms, in which chaotic dynamics are developed via a sequence of period-doubling bifurcations for decreasing f as shown in Fig. 3(a). At each period-doubling bifurcation point, the largest Lyapunov exponent approaches to zero from negative value (as shown in the lower part of Fig. 3(a)). It is noted that there is a short interval of the stable periodic oscillation in between $f = 0.1613$ and $f = 0.16149$. Around $f = 0.1613$, the size of the chaotic attractor increase dramatically. This marks the transition to spiking dynamics through a homoclinic bifurcation [6]. These chaotic dynamics end at $f = 0.1609$ with the appearance of 1:2 phase-locking rhythms via a saddle-node bifurcation. At the saddle-node bifurcation point, the largest Lyapunov exponent changes suddenly from a positive value to a negative one. The largest chaotic region (region (II)) is observed in the frequency range $0.1245 < f < 0.1311$ as shown in Fig. 3(b). It is obvious that we have positive Lyapunov exponents for the chaotic state (the lower part of Fig. 3(b)). Around $f = 0.1311$, a sudden change of the largest Lyapunov exponent

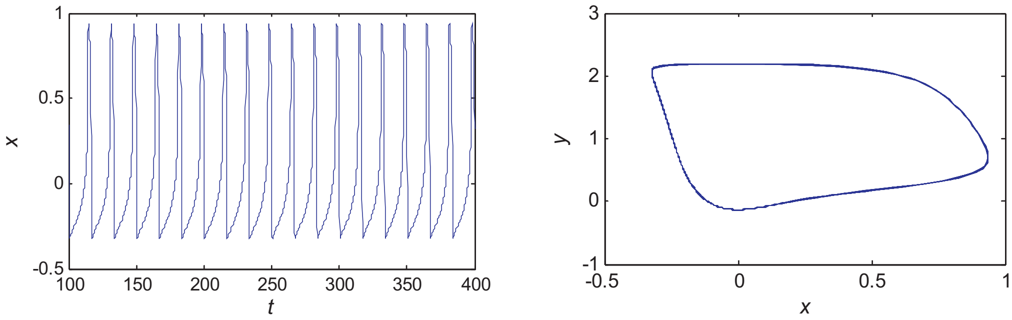

(a) 1:1 phase-locking rhythm for $f = 0.06$ and $a = 0.1$.

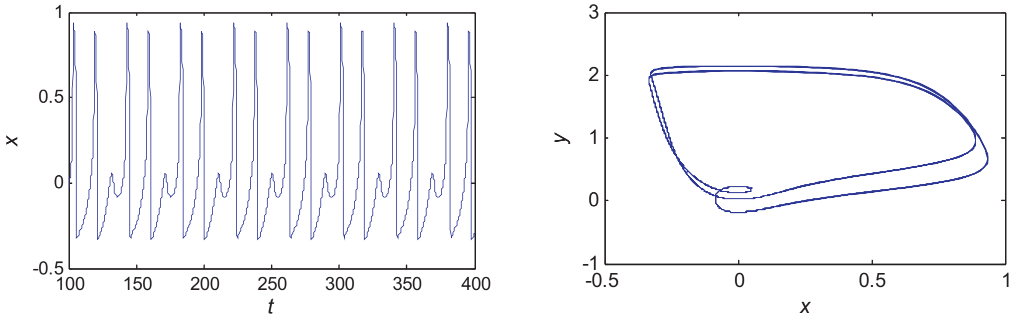

(b) 2:3 phase-locking rhythm for $f = 0.076$ and $a = 0.1$.

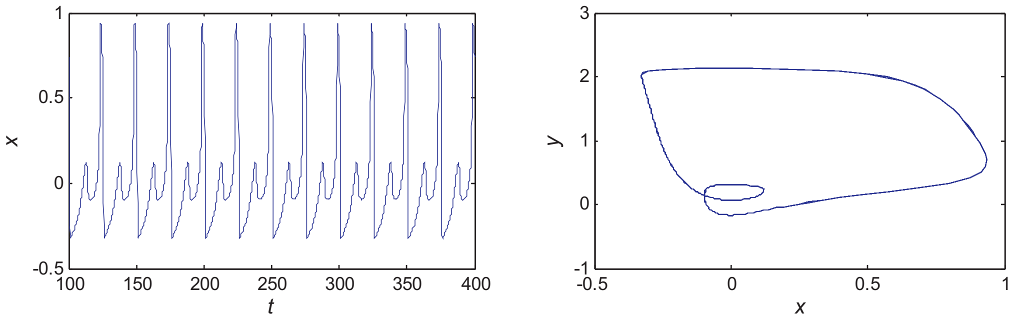

(c) 1:2 phase-locking rhythm for $f = 0.08$ and $a = 0.1$.

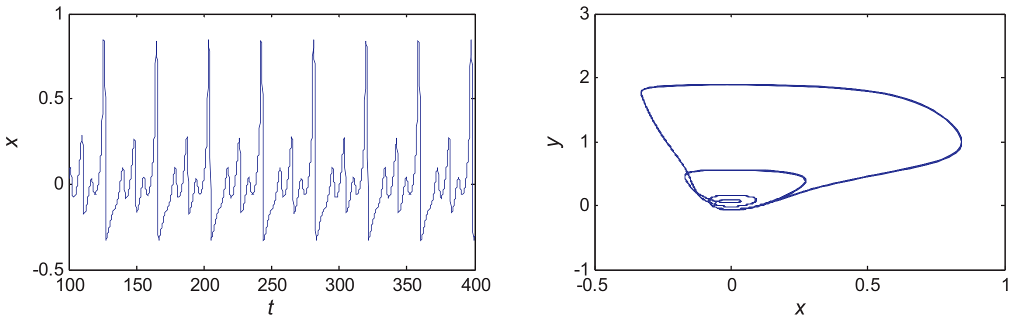

(d) 1:5 phase-locking rhythm for $f = 0.129$ and $a = 0.081$.

Fig. 1. Diverse behaviors of (1)–(2) with different values of f and a ($b_1 = 10$, $b_2 = 1.0$). All above figures were obtained after ignoring an initial transient period of 100 time units. (a) 1:1 phase-locking rhythm for $f = 0.06$ and $a = 0.1$. (b) 2:3 phase-locking rhythm for $f = 0.076$ and $a = 0.1$. (c) 1:2 phase-locking rhythm for $f = 0.08$ and $a = 0.1$. (d) 1:5 phase-locking rhythm for $f = 0.129$ and $a = 0.081$. (e) 0:1 phase-locking rhythm for $f = 0.17$ and $a = 0.081$. (f) Chaotic dynamics for $f = 0.129$ and $a = 0.1$.

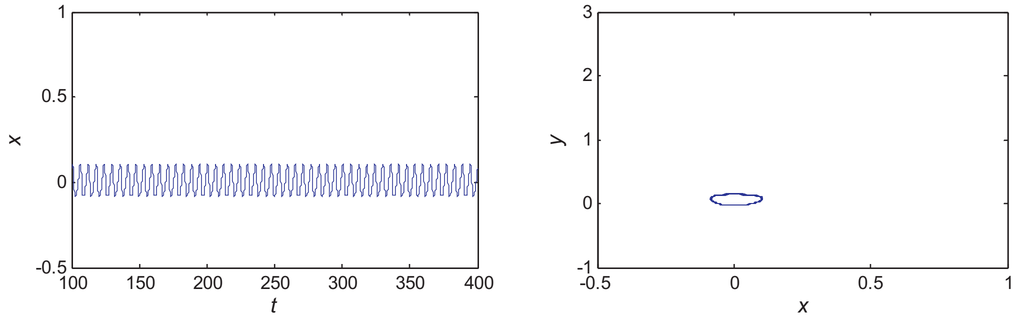

(e) 0:1 phase-locking rhythm for $f = 0.17$ and $a = 0.081$.

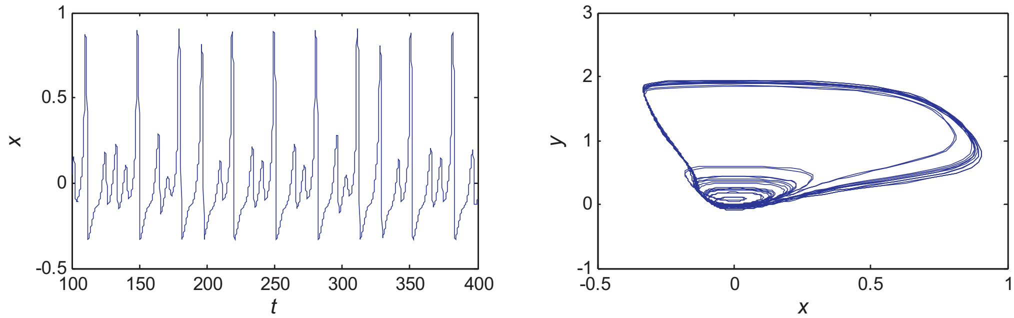

(f) Chaotic dynamics for $f = 0.129$ and $a = 0.1$.

Fig. 1. (*Continued*).

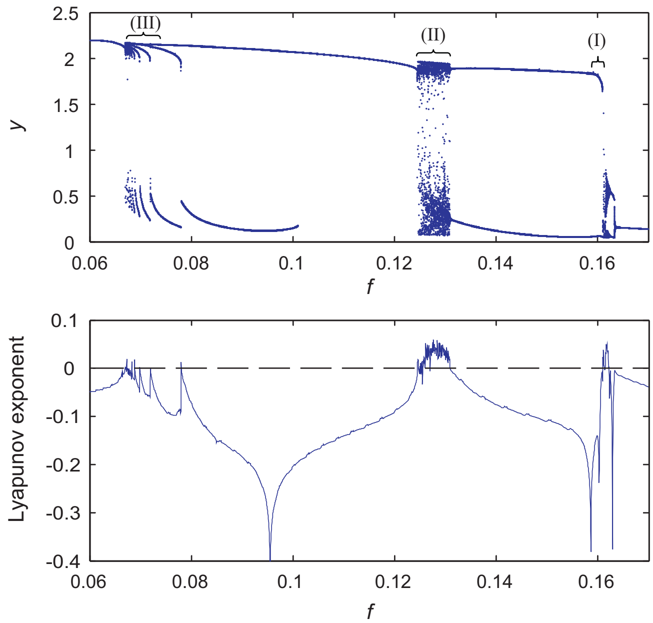

Fig. 2. The bifurcation diagram (upper) and the corresponding variation of the largest Lyapunov exponent (lower) of (1)–(2) over the frequency range, $0.06 < f < 0.17$, with $a = 0.1$, $b_1 = 10$, and $b_2 = 1.0$.

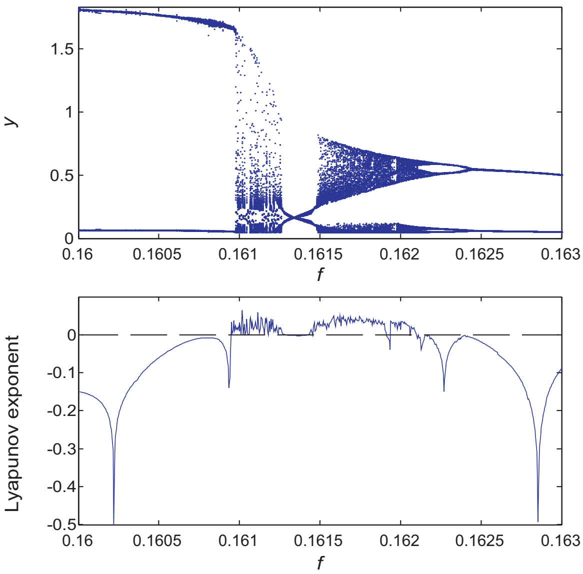

(a) Region (I) in Fig. 2, $0.160 < f < 0.163$.

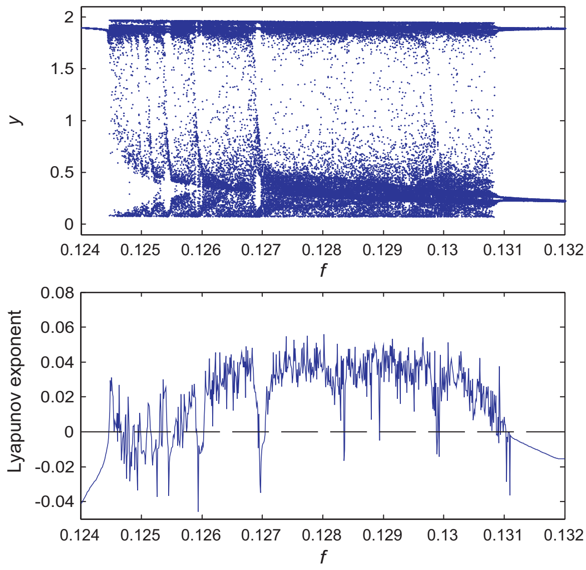

(b) Region (II) in Fig. 2, $0.124 < f < 0.132$.

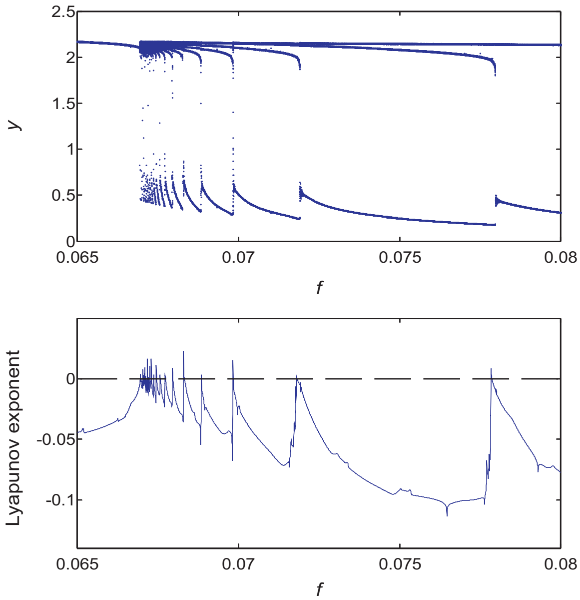

(c) Region (III) in Fig. 2, $0.065 < f < 0.080$.

Fig. 3. Three regional details from Fig. 2: bifurcation diagrams (upper) and largest Lyapunov exponents (lower).

from positive to negative takes places, the system dynamics change from chaotic to stable periodic via a saddle-node bifurcation. Finally, the last chaotic region (region (III)) occurs between 1:2 and 1:1 phase-locking rhythms for small values of f (Fig. 3(c)). In this region, we find a sequence of n:($n+1$) period-adding cascade to chaos started with $n=1$. As f is decreased further to a critical value (∼0.067), the chaotic state turns into a stable period spiking (1:1 phase-locking rhythm) through a saddle-node bifurcation. Correspondingly, the largest Lyapunov exponent becomes negative.

3. Synchronization of two coupled FHN neurons

3.1. Conditions for self-synchronization

In this subsection, the conditions for self-synchronization of two coupled FHN neurons are investigated. Based on (1), two coupled FHN neurons are modeled as

$$\frac{dx_1}{dt} = x_1(x_1 - 1)(1 - b_1 x_1) - y_1 - g(x_1 - x_2) + s(t), \tag{4a}$$

$$\frac{dy_1}{dt} = b_2 x_1, \tag{4b}$$

$$\frac{dx_2}{dt} = x_2(x_2 - 1)(1 - b_1 x_2) - y_2 - g(x_2 - x_1) + s(t), \tag{4c}$$

$$\frac{dy_2}{dt} = b_2 x_2, \tag{4d}$$

where x_i, y_i ($i = 1, 2$) are the state variables and g is the positive coupling coefficient.

Definition. The two coupled FHN neurons (4a)–(4d) are said to be globally asymptotically synchronized if, for all initial conditions $x_1(0)$, $x_2(0)$ and $y_1(0)$, $y_2(0)$, $\lim_{t\to\infty} ||x_1(t) - x_2(t)|| = 0$ and $\lim_{t\to\infty} ||y_1(t) - y_2(t)|| = 0$.

3.1.1. Sufficient condition for self-synchronization

Let $e_1 = x_2 – x_1$ and $e_2 = y_2 – y_1$ be the error signals between the states of the coupled system (4). Then the following error dynamics are derived.

$$\dot{e}_1 = [-1 - 2g + (1 + b_1)(x_1 + x_2) - b_1(x_1^2 + x_1 x_2 + x_2^2)]e_1 - e_2, \tag{5}$$

$$\dot{e}_2 = b_2 e_1. \tag{6}$$

From the definition of the global asymptotic synchronization, it is sufficient for synchronization if the trivial solution of the error dynamics (5) and (6) is globally asymptotically stable.

Theorem. *Let the coupling coefficient g satisfy the following condition:*

$$g > \frac{M[2(1 + b_1) + 3Mb_1] - 1}{2}, \tag{7}$$

where M is the upper bound of the absolute value of the membrane voltage. Then, for every initial condition ($x_1(0)$, $x_2(0)$, $y_1(0)$, $y_2(0)$)*, the two coupled FHN neurons are globally uniformly asymptotically synchronized as* $t \to +\infty$.

Proof. Note first that (0, 0) is the only equilibrium point of (5) and (6). Choose a Lyapunov function candidate as

$$E_1(e_1, e_2) = b_2 \alpha e_1^2 + \alpha e_2^2, \tag{8}$$

where α is a positive constant. The time derivative of $E_1(e_1, e_2)$ along the trajectories of (5) and (6) becomes

$$\dot{E}_1(e_1, e_2) = 2b_2 \alpha e_1 \dot{e}_1 + 2\alpha e_2 \dot{e}_2 = 2\alpha[-1 - 2g + (1 + b_1)(x_1 + x_2) - b_1(x_1^2 + x_1 x_2 + x_2^2)]e_1^2. \tag{9}$$

Since the system (4) has bounded trajectories [24], let the bound be M (i.e., $|x_1| \le M$ and $|x_2| \le M$). Thus

$$\dot{E}_1(e_1, e_2) \le -2\alpha\{1 + 2g - M[2(1 + b_1) + 3Mb_1]\}e_1^2. \tag{10}$$

Therefore, if $1 + 2g - M[2(1 + b_1) + 3Mb_1] > 0$, $\dot{E}_1(e_1, e_2) < 0$. Let $\Gamma = \{(e_1, e_2) : \dot{E}_1(e_1, e_2) = 0\}$. From (9), $\Gamma = \{(e_1, e_2)$: $e_1 = 0\}$. In the invariant set Γ, $\dot{e}_1 = 0$ holds. This again implies, by way of (5), that $e_2 = 0$. Therefore (0, 0) is the only solution in Γ. By LaSalle's theorem for periodic systems [23], we conclude that the origin is globally uniformly asymptotically stable. The proof is completed. □

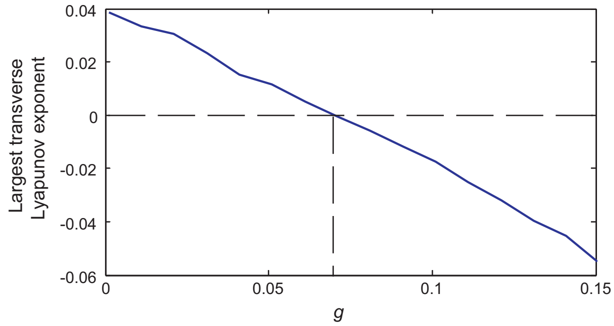

Fig. 4. λ▯ − g diagram of (4): Synchronization occurs if g becomes greater than 0.07 (b_1 = 10, b_2 = 1.0, a = 0.1, and f = 0.129).

The above theorem provides only a sufficient condition but not a necessary condition for global self-synchronization of two coupled FHN neurons. In other words, if the coupling coefficient does not satisfy (7), it does not mean that two coupled FHN neurons cannot achieve self-synchronization. In fact, numerical simulations revealed that there exist coupling coefficients that, whereas not satisfying the above sufficient condition, are adequate for synchronization of two coupled FHN neurons (see Fig. 6).

3.1.2. Necessary condition for self-synchronization

Let us introduce a new variable $z = t$. Then, the system of two coupled FHN neurons in (4) can be expressed in the following form:

$$\dot{v}_1 = f(v_1) + C(v_1 - v_2), \tag{11a}$$

$$\dot{v}_2 = f(v_2) + C(v_2 - v_1), \tag{11b}$$

where

$$v_i = \begin{bmatrix} x_i \\ y_i \\ z \end{bmatrix}, \quad f(v_i) = \begin{bmatrix} x_i(x_i - 1)(1 - b_1 x_i) - y_i + s(z) \\ b_2 x_i \\ 1 \end{bmatrix}, \quad i = 1, 2,$$

and

$$C = \begin{bmatrix} g & 0 & 0 \\ 0 & 0 & 0 \\ 0 & 0 & 0 \end{bmatrix}.$$

Define the synchronization manifold as $v_1(t) = v_2(t) = \eta(t)$. By introducing a new coordinate in the transverse direction to the synchronization manifold, $\xi(t) = v_2(t) - v_1(t)$, the linearized equation of the transversal perturbation is obtained as follows [33,34,50].

$$\delta\dot{\xi} = [Df(\eta(t)) + 2C]\delta\xi, \tag{12}$$

where

$$Df(\eta) = \begin{bmatrix} -3b_1\eta_x^2 + 2(b_1 + 1)\eta_x - 1 & -1 & -a \sin 2\pi f \eta_z \\ b_2 & 0 & 0 \\ 0 & 0 & 0 \end{bmatrix},$$

and $Df(\eta)$ denotes the Jacobian matrix of the individual neurons evaluated along the solution $\eta(t) = [\eta_x(t), \eta_y(t), \eta_z(t)]$ in the synchronization manifold.

In this paper, we adopt the necessary condition for synchronization of (4) from the literature [33,34,50], which requires that the largest transverse Lyapunov exponent is negative. So, by computing the largest Lyapunov exponent of (12), the necessity for synchronization of (4) can be verified. Fig. 4 shows the largest transverse Lyapunov exponent λ▯

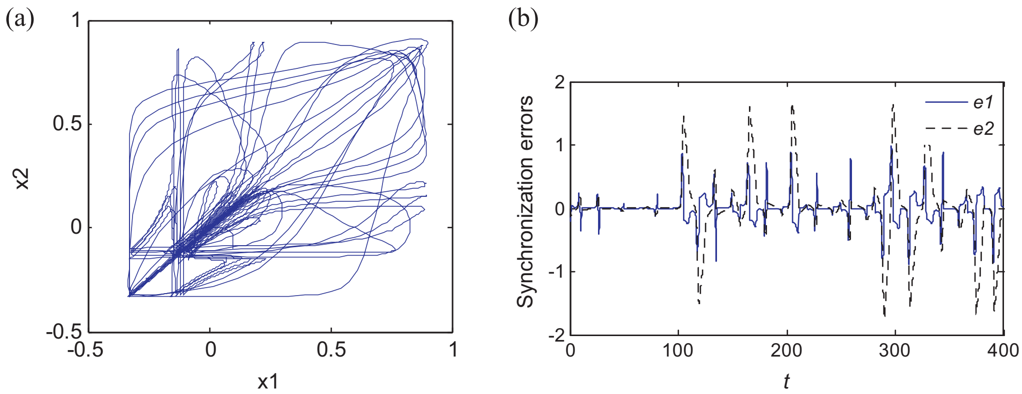

Fig. 5. Non-synchronized dynamics of (4) with $g = 0.05$: (a) x_1–x_2 phase portrait, (b) synchronization errors $e_1 = x_2 - x_1$ and $e_2 = y_2 - y_1$.

as a function of the coupling coefficient g. Here, the parameters are chosen as $b_1 = 10$, $b_2 = 1.0$, $a = 0.1$, and $f = 0.129$. As shown in Fig. 4, the synchronization threshold value is about $g = 0.07$ and, above this value, a self-synchronization of two coupled FHN neurons can occur.

It is important to note that the negativity of the largest transverse Lyapunov exponent is not a sufficient condition for the stability of the synchronized state. The reason is that there can be unstable invariant sets (e.g., fixed points, periodic orbits) with positive largest transverse Lyapunov exponents in the stable synchronization manifold. Therefore, as trajectories come near these invariant sets they can be rebelled from the synchronization manifold [20]. Some studies [5,20] have shown that the desynchronized state can appear, even when the largest transverse Lyapunov exponent is negative.

To demonstrate the effectiveness of the sufficient and the necessary conditions as well as to provide a comparison between these conditions, we simulate the coupled system (4) for different values of the coupling coefficient. Here, the parameters are chosen as $b_1 = 10$, $b_2 = 1.0$, $a = 0.1$, and $f = 0.129$. The initial condition is $(x_1(0), y_1(0), x_2(0), y_2(0)) = (0.1, 0.0, -0.1, 0.1)$. For $g = 0.05$, both conditions are not satisfied. Fig. 5 reveals that the self-synchronization cannot occur between two coupled FHN neurons. For $g = 2.0$, the sufficient condition is still not satisfied but the necessary condition holds in this case ($\lambda_{\square} = -0.2321$). It can be seen from Fig. 6 that the self-synchronization between two coupled FHN neurons can be achieved even the sufficient condition for self-synchronization does not hold.

3.2. Synchronization via a feedback control

In this section, for the case that the conditions for self-synchronization do not satisfy, a feedback control law that synchronizes the two coupled FHN neurons is developed. First, let us decompose the first terms in the right hand sides of (4a) and (4c) into two parts (linear and nonlinear) as follows.

$$\text{(I)} \quad \begin{cases} \dfrac{dx_1}{dt} = -x_1 - y_1 - g(x_1 - x_2) + (b_1 + 1)x_1^2 - b_1 x_1^3 + s(t), \\ \dfrac{dy_1}{dt} = b_2 x_1, \end{cases} \tag{13}$$

$$\text{(II)} \quad \begin{cases} \dfrac{dx_2}{dt} = -x_2 - y_2 - g(x_2 - x_1) + (b_1 + 1)x_2^2 - b_1 x_2^3 + s(t) + u, \\ \dfrac{dy_2}{dt} = b_2 x_2. \end{cases} \tag{14}$$

(I) and (II) are considered as the drive and response systems, respectively. The aim is to design the control u in (14), so that (I) and (II) are synchronized. By defining the error signals as $e_1 = x_2 - x_1$ and $e_2 = y_2 - y_1$, the error dynamics becomes

$$\dot{e}_1 = -e_1 - e_2 - 2ge_1 + (b_1 + 1)(x_2 + x_1)e_1 - b_1(x_2^2 + x_1 x_2 + x_1^2)e_1 + u, \tag{15}$$

$$\dot{e}_2 = b_2 e_1. \tag{16}$$

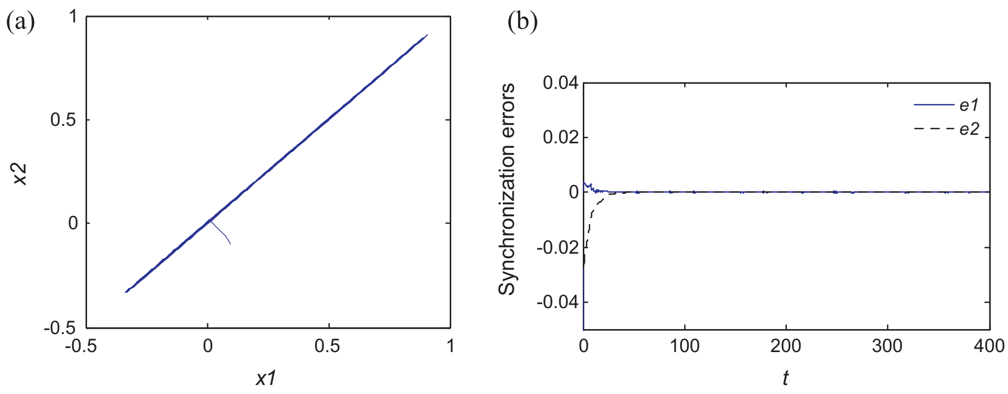

Fig. 6. Synchronization occurs when the coupling coefficient gets large ($g = 2.0$): (a) x_1–x_2 phase portrait, (b) synchronization errors $e_1 = x_2 - x_1$ and $e_2 = y_2 - y_1$.

We introduce a new term to denote the nonlinear term in (15) as

$$h(x_1, x_2, e_1) = (b_1 + 1)(x_2 + x_1)e_1 - b_1(x_2^2 + x_1x_2 + x_1^2)e_1. \tag{17}$$

Then (15) and (16) are reduced to

$$\dot{e}_1 = -e_1 - e_2 - 2ge_1 + h(x_1, x_2, e_1) + u, \tag{18}$$

$$\dot{e}_2 = b_2e_1. \tag{19}$$

The synchronization problem is replaced by finding a suitable control law u such that the asymptotical stability of the error dynamics of (18) and (19) at the origin is guaranteed.

Choose a Lyapunov function candidate as follows:

$$E_2(e_1, e_2) = e_1^2 + e_2^2. \tag{20}$$

The derivative of $E_2(e_1, e_2)$ is given by

$$\dot{E}_2(e_1, e_2) = 2e_1\dot{e}_1 + 2e_2\dot{e}_2 = -2(1 + 2g)e_1^2 + 2[h(x_1, x_2, e_1)e_1 + ue_1 - e_1e_2 + b_2e_1e_2]. \tag{21}$$

Let the control law be

$$u = -h(x_1, x_2, e_1) - (b_2 - 1)e_2. \tag{22}$$

The substitution of (22) into (21) yields

$$\dot{E}_2(e_1, e_2) = -2(1 + 2g)e_1^2 \leq 0. \tag{23}$$

Note that $\dot{E}_2(e_1, e_2) = 0$ if $e_1 = 0$. However, from (22) and (18), it is also noted that $e_2 \equiv 0$ if $e_1 \equiv 0$. Therefore, by LaSalle's theorem [23], we conclude that the origin is globally asymptotically stable. Hence, with the control law (22), the two coupled FHN neurons are globally asymptotically synchronized.

Finally, by substituting (17) into (22), the control law is rewritten as

$$u = -[(b_1 + 1)(x_2 + x_1)e_1 - b_1(x_2^2 + x_1x_2 + x_1^2)e_1] - (b_2 - 1)e_2. \tag{24}$$

To demonstrate the effectiveness of the proposed control law, numerical simulations are performed. Here, we choose the coupling coefficient $g = 0.05$ so that self-synchronization does not occur (see Fig. 5). The other parameters chosen are the same as before. Fig. 7(a) illustrates the x_1–x_2 phase portrait of the coupled neurons, which shows an immediate synchronization. Fig. 7(b) shows the convergence of the synchronization errors $e_1 = x_2 - x_1$ and $e_2 = y_2 - y_1$ to zero.

Remark 1. When the external stimulations applied to two neurons are different, say $s_1(t)$ to the drive system (I) and $s_2(t)$ to the response system (II), the control law is modified as follows:

$$u = -[(b_1 + 1)(x_2 + x_1)e_1 - b_1(x_2^2 + x_1x_2 + x_1^2)e_1] - (b_2 - 1)e_2 - [s_2(t) - s_1(t)]. \tag{25}$$

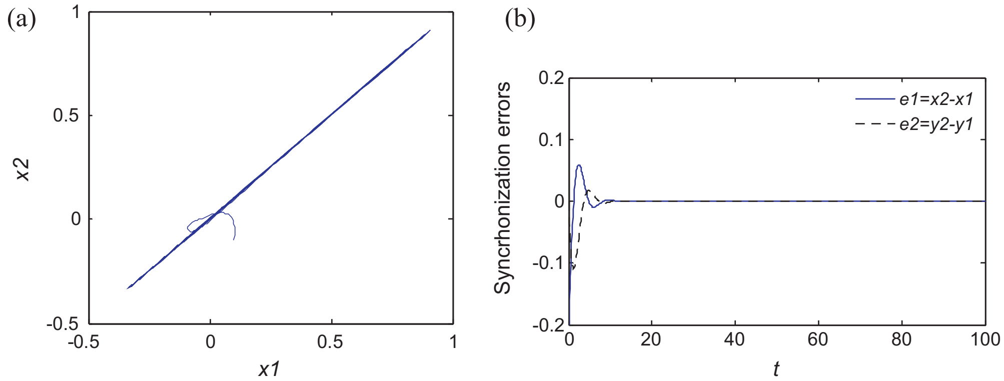

Fig. 7. Synchronization of (13) and (14) with the proposed control law (24): (a) x_1–x_2 phase portrait, (b) synchronization errors $e_1 = x_2 - x_1$ and $e_2 = y_2 - y_1$.

To demonstrate this case, the following scenarios for synchronization are pursued:

Case (1) *Frequencies are different*: We choose $f_1 = 0.135$ for the drive neuron and $f_2 = 0.129$ for the response neuron. The amplitudes of two stimulations are the same, that is, $a_1 = a_2 = 0.1$. For these parameters, the drive neuron exhibits a periodic behavior while the response neuron exhibits a chaotic behavior. The time responses of the synchronization errors and the membrane voltage of the response neuron, before and after applying the control law in (25), are shown in Fig. 8. The simulation results show that the synchronization errors converge asymptotically to zero within a finite time after the application of the control at time $t = 200$ (see Fig. 8(a)). Additionally, at the time where the control law was applied, the membrane voltage of the response neuron switches from the chaotic behavior to a periodic behavior so that it follows well the membrane voltage of the drive neuron, as shown in Fig. 8(b).

Case (2) *Amplitudes are different*: We choose $a_1 = 0.07851$ for the drive neuron and $a_2 = 0.15$ for the response neuron. The frequencies of two stimulations are the same, that is, $f_1 = f_2 = 0.129$. For these parameters, the drive neuron exhibits a chaotic behavior while the response neuron exhibits a periodic behavior. Fig. 9(a) shows the synchronization between two coupled neurons. The transition from the periodic behavior to a chaotic behavior of the response neuron's membrane voltage at the time of applying the control law in (25) is shown in Fig. 9(b).

Remark 2. The control law proposed in [15] (Eq. (14)) is given by

$$u = -[x_2(x_2 - 1)(1 - b_1 x_2) - x_1(x_1 - 1)(1 - b_1 x_1)] - (b_2 - 1)e_2. \quad (26)$$

We applied this control law to our system with exactly the same parameters and initial conditions. The comparison results are shown in Fig. 10. Clearly, our method provides much better synchronization performance. With our control law, the synchronization errors converged to zero after $t \approx 15$ (solid line), whereas $t > 100$ was spent with the control law proposed in [15] (dashed line).

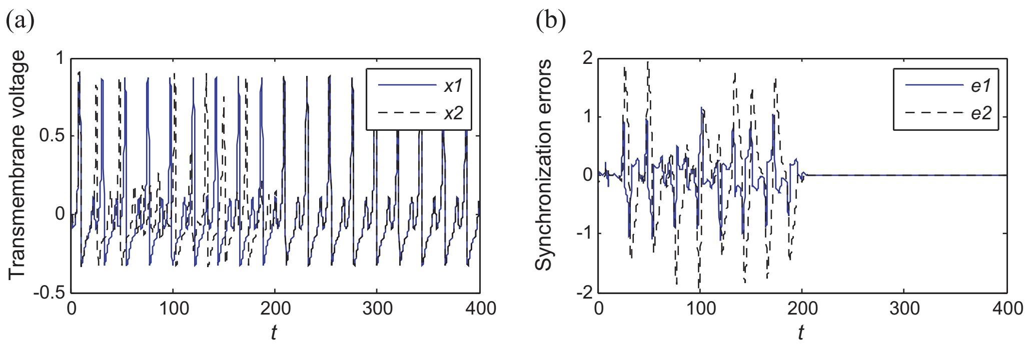

Fig. 8. Synchronization of (13) and (14) using (25) with two different frequencies ($f_1 = 0.135$ for the drive neuron and $f_2 = 0.129$ for the response neuron) at time $t = 200$: (a) membrane voltages and (b) synchronization errors.

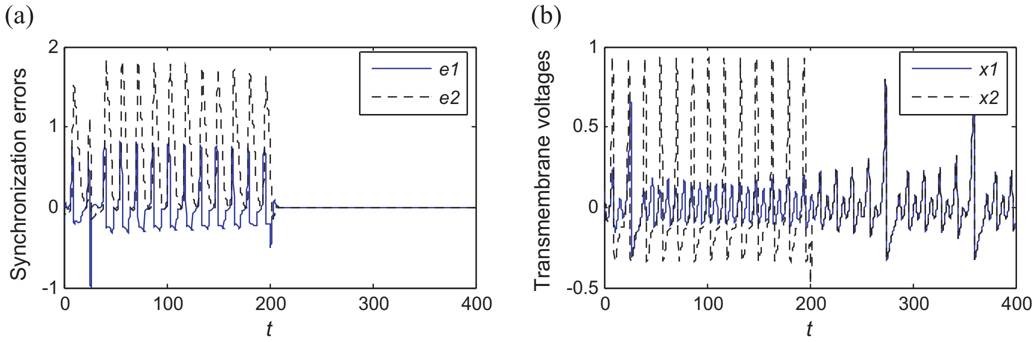

Fig. 9. Synchronization of (13) and (14) using (25) with two different amplitudes ($a_1 = 0.07851$ for the drive neuron and $a_2 = 0.15$ for the response neuron) at time $t = 200$: (a) synchronization errors and (b) membrane voltages.

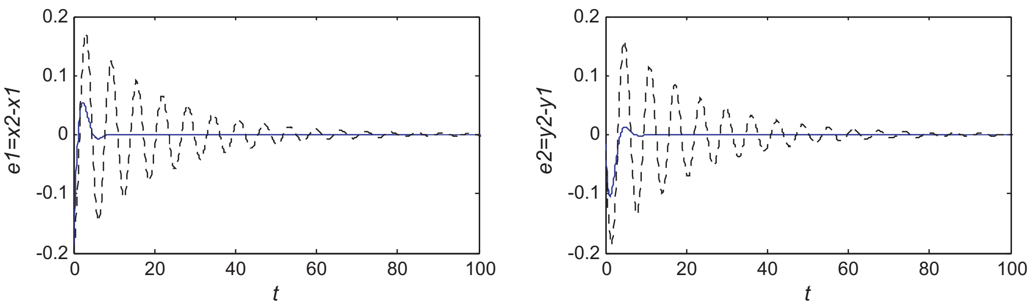

Fig. 10. Comparison of the proposed control law (24) and the law in [15] (i.e., Eq. (14)): the solid lines show the synchronization errors by (24) and the dashed lines indicate those by [15].

4. Conclusions

In this study we addressed the problem of synchronization of two chaotic FHN neurons coupled by a coupling coefficient. The synchronized state can be achieved by either a strong coupling coefficient or by a proper external control signal. In particular, we first investigated the dynamic behaviors of a single FHN neuron under various external electrical stimulations. Through simulations, three chaotic regions were specified by varying the frequency of the external electrical stimulation. Second, we established one sufficient condition and one necessary condition of the coupling coefficient for achieving self-synchronization of two coupled chaotic neurons. Also, for the case that the conditions for self-synchronization are not satisfied, we formulated a new Lyapunov function-based control law that guarantees synchronization. Neuronal synchronization, in enabling coordination between different areas in the brain, plays an important role in neural signal transmission. The present study can provide a further understanding of synchronization phenomena in a pair of biological neurons. Especially, the proposed synchronization algorithm can be a step toward the development of a synchronization scheme for a network of neurons.

Acknowledgments

This research was supported by the World Class University program through the National Research Foundation of Korea funded by the Ministry of Education, Science and Technology, Republic of Korea (Grant No. R31-20004).

References

[1] J. Aguirre, E. Mosekilde, M.A.F. Sanjuan, Analysis of the noise-induced bursting-spiking transition in a pancreatic beta-cell model, Phys. Rev. E 69 (2004) 041910.
[2] K. Aihara, G. Matsumoto, M. Ichiwaka, An alternating periodic–chaotic sequence observed in neural oscillations, Phys. Lett. A 111 (1985) 251–255.

[3] M. Aqil, K.-S. Hong, M.-Y. Jeong, Synchronization of coupled chaotic FitzHugh–Nagumo systems, Commun. Nonlinear Sci. Numer. Simul. 17 (4) (2012) 1615–1627, doi:10.1016/j.cnsns.2011.09.028.
[4] P. Ashwin, J.R. Terry, Blowout bifurcation in a system of coupled chaotic lasers, Phys. Rev. E 58 (1998) 7186–7189.
[5] P. Badola, S.S. Tambe, B.D. Kulkarni, Driving systems with chaotic signals, Phys. Rev. A 46 (1992) 6735–6737.
[6] V.N. Belykh, I.V. Belykh, M. Colding-Jørgensen, E. Mosekilde, Homoclinic bifurcations leading to the emergence of bursting oscillations in cell models, Eur. Phys. J. E 3 (2000) 205–219.
[7] S. Boccaletti, J. Kurths, G. Osipov, D.L. Valladares, C.S. Zhou, The synchronization of chaotic systems, Phys. Rep. 336 (2002) 1–101.
[8] S. Bowong, M. Kakmeni, R. Koina, Chaos synchronization and duration time of a class of uncertain chaotic systems, Math. Comput. Simul. 71 (3) (2006) 212–228.
[9] H.A. Braun, H. Wissing, K. Schäfer, M.C. Hirsch, Oscillation and noise determine signal transduction in shark multimodel sensory cells, Nature 367 (1994) 270–273.
[10] J.M. Casado, Synchronization of two Hodgkin–Huxley neurons due to internal noise, Phys. Lett. A 310 (2003) 400–406.
[11] T.R. Chay, Chaos in a three-variable model of an excitable cell, Physica D16 (1985) 233–242.
[12] M.H. Chou, Y.T. Lin, Exotic dynamic behavior of the forced FitzHugh–Nagumo equations, Comput. Math. Appl. 32 (1996) 109–124.
[13] S. Coombes, A.H. Osbaldestin, Period-adding bifurcations and chaos in a periodically stimulated excitable neural relaxation oscillator, Phys. Rev. E 62 (2000) 4057–4066.
[14] O. Cornejo-Pérez, R. Femat, Unidirectional synchronization of Hodgkin–Huxley neurons, Chaos Soliton Fract. 25 (2005) 43–53.
[15] B. Deng, J. Wang, X. Fei, Synchronizing two coupled chaotic neurons in external electrical stimulation using backstepping control, Chaos Soliton Fract. 29 (2006) 182–189.
[16] E. Eckhorn, Neural mechanisms of scene segmentation: recording from the visual cortex suggests basic circuits or linking field models, IEEE Trans. Neural Netw. 10 (1999) 464–479.
[17] Y.-S. Fan, T.R. Chay, Generation of periodic and chaotic bursting in an excitable cell model, Biol. Cybern. 71 (1984) 417–431.
[18] R. Fitzhugh, Thresholds and plateaus in the Hodgkin–Huxley nerve equations, J. Gen. Physiol. 43 (1960) 867–896.
[19] M.R. Guevara, L. Glass, A. Shrier, Phase locking, period-doubling bifurcation, and irregular dynamics in periodically stimulated cardiac cells, Science 214 (1981) 1350–1353.
[20] J.F. Heagy, T.L. Carroll, L.M. Pecora, Desynchronization by periodic orbits, Phys. Rev. E 52 (1995) 1253–1256.
[21] J.L. Hindmarsh, R.M. Rose, A model of neuronal bursting using three coupled first order differential equations, Proc. R. Soc. Lond. B 221 (1984) 87–102.
[22] A.L. Hodgkin, A.F. Huxley, A quantitative description of membrane current and its application to conduction and excitation in nerve, J. Physiol. 117 (1952) 500–544.
[23] H.K. Khalil, Nonlinear Systems, third ed., Prentice Hall, New York, 2002.
[24] T. Kostova, R. Ravindran, M. Schonbek, FitzHugh–Nagumo revisited: types of bifurcations, periodical forcing and stability regions by a Lyapunov functional, Int. J. Bifurcat. Chaos 14 (3) (2004) 913–925.
[25] G.M. Mahmoud, E.E. Mahmoud, Synchronization and control of hyperchaotic complex Lorenz system, Math. Comput. Simul. 80 (12) (2010) 2286–2296.
[26] G. Matsumoto, K. Aihara, M. Ichikawa, A. Tasaki, Periodic and nonperiodic response of membrane potentials in squid giant axons during sinusoidal current stimulation, J. Theoret. Neurobiol. 3 (1984) 1–14.
[27] C. Morris, H. Lecar, Voltage oscillations in the barnacle giant muscle fiber, Biophys. J. 35 (1981) 193–213.
[28] E. Mosekilde, A.L. Fradkov, I.I. Blekhman, Chaos synchronization and control-Preface, Math. Comput. Simul. 58 (4–6) (2002) 283–284.
[29] E. Mosekilde, B. Lading, S. Yanchuk, Y. Maistrenko, Bifurcation structure of a model of bursting pancreatic cells, BioSystems 63 (2001) 3–13.
[30] J. Nagumo, S. Arimoto, S. Yoshizawa, An active pulse transmission line simulating nerve axon, Proc. IRE 50 (1962) 2061–2070.
[31] A.B. Neiman, D.F. Russell, Synchronization of noise-induced bursts in noncoupled sensory neurons, Phys. Rev. Lett. 88 (2002) 138103.
[32] E. Ott, J.C. Sommerer, Blowout bifurcations: the occurrence of riddled basins and on–off intermittency, Phys. Lett. A 188 (1994) 39–47.
[33] L.M. Pecora, T.L. Carroll, Master stability functions for synchronized coupled systems, Phys. Rev. Lett. 80 (1998) 2109–2112.
[34] L.M. Pecora, T.L. Carroll, Synchronization in chaotic systems, Phys. Rev. Lett. 64 (1990) 821–825.
[35] R.E. Plant, Bifurcation and resonance in a model for bursting nerve cells, J. Math. Biol. 11 (1981) 15–32.
[36] D.E. Postnov, L.S. Ryazanova, E. Mosekilde, O.V. Sosnovtseva, Neural synchronization via potassium signaling, Int. J. Neural Syst. 16 (2) (2006) 99–109.
[37] D.E. Postnov, L.S. Ryazanova, R.A. Zhirin, E. Mosekilde, O.V. Sosnovtseva, Noise controlled synchronization in potassium coupled neural models, Int. J. Neural Syst. 17 (2) (2007) 105–113.
[38] M. Rehan, K.-S. Hong, M. Aqil, Synchronization of multiple chaotic FitzHugh–Nagumo neurons with gap junctions under external electrical stimulation, Neurocomputing 74 (16) (2011) 3296–3304.
[39] M. Rehan, K.-S. Hong, LMI-based robust adaptive synchronization of FitzHugh–Nagumo neurons with unknown parameters under certain external electrical stimulation, Phys. Lett. A 375 (15) (2011) 1666–1670.
[40] M.G. Rosenblum, A.S. Pikovsky, J. Kurths, Phase synchronization of chaotic oscillators, Phys. Rev. Lett. 76 (1996) 1804–1807.
[41] N.F. Rulkov, M.M. Sushchik, Robustness of synchronized chaotic oscillations, Int. J. Bifurcat. Chaos 7 (1997) 625–643.
[42] N.F. Rulkov, M.M. Sushchik, L.S. Tsimring, Generalized synchronization of chaos in directionally coupled chaotic systems, Phys. Rev. E 51 (1995) 980–994.
[43] H. Salarieh, A. Alasty, Adaptive chaos synchronization in Chua's systems with noisy parameters, Math. Comput. Simul. 79 (3) (2008) 233–241.
[44] C.J. Thompson, D.C. Bardos, Y.S. Yang, K.H. Yoyner, Nonlinear cable models for cell exposed to electric field I. General theory and space-clamped solutions, Chaos Soliton Fract. 10 (11) (1999) 1825–1842.

[45] L.L. Tian, D.H. Li, X.F. Sun, Nonlinear-estimator-based robust synchronization of Hodgkin–Huxley neurons, Neurocomputing 72 (2008) 186–196.
[46] X.J. Wan, J.T. Sun, Adaptive–impulsive synchronization of chaotic systems, Math. Comput. Simul. 81 (8) (2011) 1609–1617.
[47] J. Wang, Z. Zhang, H. Li, Synchronization of FitzHugh–Nagumo systems in EES via H-infinity variable universe adaptive fuzzy control, Chaos Soliton Fract. 36 (2008) 1332–1339.
[48] A. Wolf, J.B. Swift, H.L. Swinney, J.A. Vastano, Determining Lyapunov exponents from a time series, Physica D 16 (1985) 285–317.
[49] C.W. Wu, L.O. Chua, A unified framework for synchronization and control of dynamical system, Int. J. Bifurcat. Chaos 10 (1994) 979–998.
[50] S. Yanchuk, Y. Maistrenko, B. Lading, E. Mosekilde, Effects of a parameter mismatch on the synchronization of two coupled chaotic oscillators, Int. J. Bifurcat. Chaos 10 (2000) 2629–2648.